HEP/123-qed

Dimensionality Effects on the Su-Schrieffer-Heeger Model

Marco Zoli

Istituto Nazionale Fisica della Materia - Universitá di Camerino,

62032 Camerino, Italy. e-mail: zoli.marco@libero.it

(February 1, 2008)

Abstract

A low order diagrammatic study of the dimension dependent Su-Schrieffer-Heeger model Hamiltonian in the weak electron-phonon coupling regime is presented. Exact computation of both the charge carrier effective mass and the electron spectral function shows that electrons are good quasiparticles in the antiadiabatic limit but new features emerge in the adiabatic and intermediate regime, where the phonons and the electrons compare on the energy scale. Here we find: i) a sizeable mass enhancement over the bare band value, ii) the appearance of many transition peaks in the band bottom spectral function together with a growing loss of spectral weight at larger *e-ph* couplings. The onset of a polaronic state is favoured in two dimensions.

keywords: Adiabatic Polarons, Effective Mass, Electron-Phonon Coupling
PACS: 63.20.Dj, 71.18.+y, 71.38.+i

1.INTRODUCTION

A sizeable electron-phonon interaction can induce a local deformation in the lattice structure accompanied by the formation of a quasiparticle with multiphononic character, the polaron [1]. A wide literature has been produced on the subject during the last decades [2–8] and particular emphasis has been recently laid on the polaronic properties of high T_c superconductors [9]. As the spatial extension of the lattice deformation can vary, the concepts of large and small polaron have been introduced: the transition between a large and a small polaron state is driven by the strength of the electron-phonon coupling [10–13] and monitored through the behavior of ground state properties such as the polaron energy band and the effective mass [14–16]. This transition [17], leading to a self trapped state [18] at strong couplings, is accompanied by a sizeable enhancement of the effective mass whose value may change considerably according to the degree of adiabaticity and the peculiarities of the lattice structure [19,20]. Theoretical investigations usually start from the Holstein molecular crystal model [21] which assumes a momentum independent coupling of electrons to dispersive optical phonons. The coupling to acoustical phonons, although possible in principle [20], would lead to huge mass renormalizations [22]. In fact, also the Holstein optical polaron masses are very heavy (at least larger than 10^3 times the bare band mass) in the self-trapped state but masses of order 10 times the bare band mass are possible in the presence of high energy phonon spectra [23]. As a remarkable feature of the Holstein model the polaron mass turns out to be essentially dimension independent for any value of the adiabaticity parameter [24].

In some systems however [25–27] the *e-ph* interaction modifies the electron hopping matrix elements thus leading to a momentum dependent coupling function. In this case an appropriate theoretical framework is offered by the Su-Schrieffer-Heeger(SSH) model Hamiltonian [28] originally proposed to explain the conducting properties of quasi one dimensional polymers as polyacetylene [29]. In these systems the CH monomers form chains of alternating double and single bonds leading to two regions with different structural patterns having

the same energy. This twofold degenerate ground state sustains a nonlinear localized excitation, a domain wall separating the two regions. Being the wall thickness much larger than the lattice constant in the weak coupling regime a continuum version [30] of the SSH model has been formulated thus leading to an analytical description of the solitonic excitation in the dimerized system [31]. The continuum model admits also polaron-like solutions [32–34] and a periodic array of solitons solution, the soliton lattice [35,36].

In general, the SSH Hamiltonian provides an alternative (to the Holstein model) tool to analyse the physics of polaron formation as tuned by the strength of the *e-ph* coupling. In two dimensions, the SSH model has also been studied as a particular case of the 2D half filled Hubbard model (with zero on site repulsion) [37] soon after the discovery of high T_c superconductivity. In particular, a recent investigation [38] has revealed the complexity of the square lattice structure described by a SSH type Hamiltonian pointing out that the opening of the gap at the Fermi level (due to the Peierls distortion) involves many lattice modes with wave numbers parallel to the nesting vector. The static and dynamical polaronic properties have been also analysed [39] in the same model and estimates of the effective mass have suggested that 2D polarons are heavier than 1D polarons.

This paper deals with the two dimensional electron-lattice system treating the SSH tight binding Hamiltonian by a weak coupling perturbative method. This approach, although not adequate to capture the full multiphononic nature of the polaronic quasiparticle, still can provide useful informations [40] regarding the onset of polaron formation in some portions of parameter space. Here we look first at the mass renormalization in one and two dimensions exploring a wide range of values for the adiabatic parameter and, successively, we compute the electronic spectral function to detect whether and to which extent bare electrons behave as good quasiparticles. The Section 2 outlines the SSH model and contains the results of this study while some conclusions are drawn in Section 3.

2.MODEL AND RESULTS

In real space the SSH Hamiltonian reads

$$
\begin{aligned}
H = & \sum_{\mathbf{r},\mathbf{s}} J_{\mathbf{r},\mathbf{r+s}}(f^{\dagger}_{\mathbf{r}} f_{\mathbf{r+s}} + f^{\dagger}_{\mathbf{r+s}} f_{\mathbf{r}}) + \sum_{\mathbf{r}} \Big(\frac{p^2_{\mathbf{r}}}{2M} + \sum_{\mathbf{r},\mathbf{s}} \frac{K}{2} (u_{\mathbf{r}} - u_{\mathbf{r+s}})^2 \Big) \\
J_{\mathbf{r},\mathbf{r+s}} = & -\frac{1}{2}[J + \alpha(u_{\mathbf{r}} - u_{\mathbf{r+s}})]
\end{aligned}
\tag{0.1}
$$

where the double summation over $\mathbf{r}$ and $\mathbf{s}$ runs over first neighbors lattice sites. J is the nearest neighbors hopping integral and isotropic conditions are assumed in the square lattice. α is the electron-phonon coupling, $u_{\mathbf{r}}$ is the dimerization coordinate which specifies the displacement of the $\mathbf{r}-$ lattice site from the equilibrium position, $p_{\mathbf{r}}$ is the momentum operator conjugate to $u_{\mathbf{r}}$, M is the ion (ionic group) mass, K is the effective spring constant, $f^{\dagger}_{\mathbf{r}}$ and $f_{\mathbf{r}}$ create and destroy electrons on the $\mathbf{r}-$ site. Let's expand the lattice displacement and its conjugate momentum in terms of the phonon creation and annihilation operators $b^{\dagger}_{\mathbf{q}}$ and $b_{\mathbf{q}}$ and Fourier transform the electron operators

$$
\begin{aligned}
u_{\mathbf{r}} = & \sum_{\mathbf{q}} \frac{1}{\sqrt{2MN\omega_{\mathbf{q}}}} (b^{\dagger}_{-\mathbf{q}} + b_{\mathbf{q}}) \exp(i\mathbf{q}\cdot\mathbf{r}) \\
p_{\mathbf{r}} = & \; i \sum_{\mathbf{q}} \sqrt{\frac{M\omega_{\mathbf{q}}}{2N}} (b^{\dagger}_{-\mathbf{q}} - b_{\mathbf{q}}) \exp(i\mathbf{q}\cdot\mathbf{r}) \\
f_{\mathbf{r}} = & \; \frac{1}{\sqrt{N}} \sum_{\mathbf{k}} \exp(i\mathbf{k}\cdot\mathbf{r}) f_{\mathbf{k}}
\end{aligned}
\tag{0.2}
$$

in order to obtain the SSH Hamiltonian in momentum space:

$$
\begin{aligned}
H = & \; H_0 + H_{int} \\
H_0 = & \sum_{\mathbf{k}} \varepsilon_{\mathbf{k}} f^{\dagger}_{\mathbf{k}} f_{\mathbf{k}} + \sum_{\mathbf{q}} \omega_{\mathbf{q}} b^{\dagger}_{\mathbf{q}} b_{\mathbf{q}} \\
H_{int} = & \sum_{\mathbf{k},\mathbf{q}} g(\mathbf{k}+\mathbf{q},\mathbf{k}) (b^{\dagger}_{-\mathbf{q}} + b_{\mathbf{q}}) f^{\dagger}_{\mathbf{k}+\mathbf{q}} f_{\mathbf{k}} \\
\varepsilon_{\mathbf{k}} = & \; -J\cos(\mathbf{k}\cdot\mathbf{a}) \\
\omega^2_{\mathbf{q}} = & \; 4\frac{K}{M}\sin^2\Big(\frac{\mathbf{q}\cdot\mathbf{a}}{2}\Big) \\
g(\mathbf{k}+\mathbf{q},\mathbf{k}) = & \; \frac{i\alpha}{\sqrt{2MN\omega_{\mathbf{q}}}} (\sin((\mathbf{k}+\mathbf{q})\cdot\mathbf{a}) - \sin\mathbf{k}\cdot\mathbf{a})
\end{aligned}
\tag{0.3}
$$

where N is the total number of lattice sites. $a = |\mathbf{a}|$ is the lattice constant and the 2D reduced Brillouin zone is spanned by the vectors $\mathbf{b}_1 = (2\pi/a, 0)$ and $\mathbf{b}_2 = (0, 2\pi/a)$. Being $\mathbf{q} = (q_x, q_y)$, the numerical integration constraint is defined by $q_x \in [0, 2\pi/a]$, $q_y \in [0, 2\pi/a - q_x]$. In 1D, the phonon dispersion relation is defined in the range $q \in [0, \pi]$ and, in the reduced Brillouin zone, the spectrum displays both an acoustic and an optical branch [41]. The model contains three free parameters: the hopping integral J, the zone boundary frequency $\omega_\pi = 2\sqrt{K/M}$ which coincides with the zone center optical frequency in the reduced zone scheme, the coupling constant $\alpha^2/4K$.

The full electron propagator in the Matsubara Green's functions formalism is defined as:

$$G(\mathbf{k}, \tau) = -\sum_{n=0}^{\infty}(-1)^n \int_0^\beta d\tau_1 ... d\tau_n \Big\langle T_\tau f_{\mathbf{k}}(\tau) H_{int}(\tau_1) \cdot \cdot H_{int}(\tau_n) f_{\mathbf{k}}^\dagger(0) \Big\rangle_0 \tag{0.4}$$

where β is the inverse temperature, T_τ is the time ordering operator, $< ... >_0$ indicates that thermodynamic averages are taken with respect to the unperturbed Hamiltonian and only different connected diagrams contribute to any order n. I have computed exactly the self-energy terms due to one phonon ($n = 2$ in eq.(4)) and two phonons ($n = 4$ in eq.(4)) scattering processes which determine the renormalized electron mass m_{eff} through the relations:

$$\frac{m_{eff}}{m_0} = \frac{1 - \partial Re\Sigma_{\mathbf{k}}(\epsilon)/\partial\epsilon|_{\mathbf{k}=0;\ \epsilon=-J}}{1 + \partial Re\Sigma_{\mathbf{k}}(\epsilon)/\partial\varepsilon_{\mathbf{k}}|_{\mathbf{k}=0;\ \epsilon=-J}} \tag{0.5}$$

where, $Re\Sigma_{\mathbf{k}}(\epsilon) = Re\Sigma_{\mathbf{k}}^{(1)}(\epsilon) + Re\Sigma_{\mathbf{k}}^{(2a)}(\epsilon) + Re\Sigma_{\mathbf{k}}^{(2b)}(\epsilon) + Re\Sigma_{\mathbf{k}}^{(2c)}(\epsilon)$ is the frequency dependent real part of the retarded self-energy. There are three contributions due to different connected two-phonons diagrams [42]. Their effect is however confined to the intermediate regime in which ω_π is comparable to the electronic energy J. We set $J = 0.1eV$ with the caveat that electron-electron correlations (weak in conducting polymers with wide π-electron bands and not taken into account by the SSH model) may become relevant in narrow band systems. This value is lower than those usually taken for the SSH adiabatic model but it allows us to discuss also a broad range of (anti)adiabatic parameters with reasonable choices of phonon energies. In the intermediate regime, the two phonons diagrams enhance

the effective mass by $\sim 15\%$ with respect to the one phonon result. Instead, in the fully adiabatic and antiadiabatic regimes the two phonons contributions (evaluated at the band bottom) are negligible. Hereafter, the displayed results depend on the very one phonon self-energy $\Sigma^{(1)}_{\mathbf{k}}(i\epsilon_m)$ term ($\epsilon_m = (2m+1)\pi/\beta$ with m integer number) whose finite temperatures analytic expression is given by:

$$\Sigma^{(1)}_{\mathbf{k}}(i\epsilon_m) = -\sum_{\mathbf{q}} g^2(\mathbf{k}, \mathbf{k}-\mathbf{q}) \left[\frac{n_B(\omega_{\mathbf{q}}) + n_F(-\varepsilon_{\mathbf{k}-\mathbf{q}})}{i\epsilon_m - \varepsilon_{\mathbf{k}-\mathbf{q}} - \omega_{\mathbf{q}}} + \frac{n_B(\omega_{\mathbf{q}}) + n_F(\varepsilon_{\mathbf{k}-\mathbf{q}})}{i\epsilon_m - \varepsilon_{\mathbf{k}-\mathbf{q}} + \omega_{\mathbf{q}}} \right] \tag{0.6}$$

n_B and n_F are the Bose and Fermi occupation factors respectively.

Figure 1 shows, both in one and two dimensions, a sizeable mass enhancement in the intermediate regime with a pronounced spike at $\omega_\pi \sim \sqrt{2}J$. In 2D the effective mass is larger than in 1D. The onset of a mass renormalization starting at $\omega_\pi \sim J/2$ and, more evidently, at $\omega_\pi \sim J$ (together with the increased relevance of multiphonons contributions) signals that polaron formation is expected in this regime while no mass enhancement is obtained in the adiabatic and antiadiabatic limits. The same trend is observed both in 1D and 2D. Let's analyse in detail the origin of the divergent-like mass behavior. The main contribution to both self-energy partial derivatives in eq.(5) comes from the lattice mode vectors connecting two electronic states such that $J + \varepsilon_{\mathbf{q}} - \omega_{\mathbf{q}} \sim 0$ hence, from $\mathbf{q}$-vectors satisfying the relation

$$\frac{J\sqrt{2}}{\omega_\pi} \sim \sqrt{1 - cos(\mathbf{q}\cdot\mathbf{a})}$$

Although for any value $J < \omega_\pi$ a set of singular $\mathbf{q}$-vectors does exist, their divergent contributions to the numerator and denominator in eq.(5) generally cancel out and no substantial effect is seen on the effective mass. Only in the case $\omega_\pi \sim \sqrt{2}J$ something special occurs due to scattering by phonons at the points such that $|q_x + q_y| = \pi/2$. Infact $\partial Re\Sigma_{\mathbf{k}}(\epsilon)/\partial\varepsilon_{\mathbf{k}}$ contains as modulation factor a $cos(\mathbf{q}\cdot\mathbf{a})$ term which is peculiar of the band structure and responsible for the van Hove singularities in the density of states. The vanishing of this term at the same wave vectors which allow for energy conservation finally results in the abrupt increase of the effective mass observed in Fig.1. In the square lattice the divergent-like behavior is more evident since many points (only one point in 1D) fulfill the simultaneous

occurence of the two singular effects. It should be emphasized that this phenomenon, rather than being a general feature of two dimensional systems, is related to the peculiarities of the electron band in the square lattice.

Let's look now at the spectral function defined by $A(\mathbf{k},\,\epsilon) = -2ImG_{ret}(\mathbf{k},\,\epsilon)$ to get more insight [43] into the suggestions proposed by the effective mass behavior. In terms of the retarded self-energy, obtained by eq.(6) through analytic continuation $\epsilon_m \to \epsilon + i\delta$, $A(\mathbf{k},\,\epsilon)$ reads:

$$A(\mathbf{k},\,\epsilon) = 2\pi\delta(\epsilon - \varepsilon_{\mathbf{k}} - Re\Sigma_{\mathbf{k}}(\epsilon)) + \frac{(-)2Im\Sigma_{\mathbf{k}}(\epsilon)}{\Big(\epsilon - \varepsilon_{\mathbf{k}} - Re\Sigma_{\mathbf{k}}(\epsilon)\Big)^2 + \Big[Im\Sigma_{\mathbf{k}}(\epsilon)\Big]^2} \tag{0.7}$$

The first addendum in eq.(7) contributes when $Im\Sigma_{\mathbf{k}}(\epsilon) = 0$. The band bottom ($|\mathbf{k}| = 0$) spectral function has been computed in a number of representative cases and numerical convergence has been achieved by summing the self-energy term (eq.(6)) over 6000 $q-$points in the 1D Brillouin zone and 90000 $\mathbf{q}-$ points in the reduced 2D Brillouin zone. The complexity of the numerical work is mainly related to the search of the zeros of the δ-function argument in eq.(7) and in the $Im\Sigma_{k=0}(\epsilon)$. In 1D, we have used the representation

$$\delta[f(q)] = \frac{\delta(q - q^0)}{|df/dq|_{q=q^0}}$$

and obtained convergence by summing over 10^5 points of the $\epsilon-$ axis. In 2D, the sum over $\mathbf{q}$ vectors can be handled as follows:

$$\frac{1}{N}\sum_{\mathbf{q}} \to \frac{1}{N_x}\sum_{q_x}\sqrt{V}\int_{-\infty}^{\infty}\frac{dq_y}{2\pi}$$

with V being the cell volume and, at a fixed q_x, the δ-function transforms as

$$\delta[f(q_x,q_y)] = \frac{\delta(q_y - q_y^0)}{|\partial f/\partial q_y|_{q_y=q_y^0}}.$$

At any ϵ (we take 80000 points) the program searches the (q_x,q_y) points which allow for energy conservation and the $Im\Sigma_{k=0}(\epsilon)$ is normalized over the total number of these pairs.

The sum rule

$$\int_{-\infty}^{\infty}\frac{d\epsilon}{2\pi}A(|\mathbf{k}| = 0,\,\epsilon) = 1$$

has to be numerically fulfilled in principle. Here however we are approximating the total self-energy by the one-phonon term (eq.(6)) which linearly depends on the free parameter $\alpha^2/4K$. As the *e-ph* coupling grows multiphonons terms become more relevant and our approximation becomes less accurate. Accordingly, deviations from the sum rule are expected as a measure of the loss of spectral weight associated with higher order self-energy effects. In this regard, the sum rule numerical analysis permits to define the range of $\alpha^2/4K$ values within which the one phonon approximation is reliable. For any choice of input parameters we are able to estimate the intrinsic error of our physical model.

Let's start the discussion looking at the spectral function in the adiabatic regime (Figures 2). In one dimension and at very weak coupling (Fig.2(a)) the sum rule is satisfied and the spectral weight spreads mainly in a few peaks around the highest one located at the energy $\epsilon = -100meV$ with a significant tail up to energy levels of order $\epsilon \sim -80meV$. At larger couplings (Fig.2(c)), where the dimensionless effective coupling is $\alpha^2/(4KJ) = 0.1$, the tail is appreciable up to $\epsilon \sim -50meV$ and the loss of spectral weight is $\sim 20\%$, being $\int_{-\infty}^{\infty} d\epsilon A(k = 0, \epsilon)/2\pi = 0.8$. A well defined transition is however still present at $\epsilon = -108.2meV$. In two dimensions, a few well resolved transitions around $\epsilon = -100meV$ show up at very weak couplings (Fig.2(b)) and the sum rule is again satisfied but the loss of spectral weight grows to $\sim 50\%$ at larger couplings (Fig.2(d)). The breakdown of the one phonon approximation is therefore dimension dependent and, by increasing the *e-ph* coupling, 2D systems seem to favour the appearance of multiphononic contributions in the adiabatic regime.

Figures 3 deal with the intermediate regime $\omega_\pi = J$. Electrons are still good excitations in the extremely weak coupling and one dimensional case (Fig. 3(a)) with one well defined transition at $\epsilon = -100.9meV$ but, at larger couplings (Fig. 3(c)), the sum rule is far from being satisfied and a 40% loss of spectral weight is observed together with a strong reduction of the main peak height whose position is shifted to $\epsilon = -119meV$. In 2D, the sum rule is fulfilled at very weak couplings (Fig. 3(b)) but the appearance of several transitions peaks in the range $[-110, -90]meV$ signals the onset of a polaronic state. At larger couplings (Fig. 3(d)) the sum rule is strongly violated and the electronic quasiparticle picture totally

breaks down. Note that the absorption spectra broaden (both in 1D and 2D) by enhancing the strength of the *e-ph* coupling as a consequence of the mixing of electronic states and lattice vibrational excitations. Although comparisons with specific data are not possible at this stage, broad photoemission spectra are known [7,19,44] to be a feature of systems with polaronic charge carriers.

Figures 4 illustrate that electrons are good quasiparticles in the fully antiadiabatic regime in one and also in two dimensions. In 1D, for both values of the *e-ph* coupling there is a well resolved peak due to the $\delta-$function contribution and located at $\epsilon = -98.8meV$ (Fig. 4(a)) and $\epsilon = -90.4meV$ (Fig. 4(c)), respectively. The sum rule is well satisfied in Fig. 4(a) while a slight loss of spectral weight occurs in Fig. 4(c) being $\int_{-\infty}^{\infty} d\epsilon A(k = 0, \epsilon)/2\pi = 0.92$. In 2D the spectra do not exhibit any relevant change with respect to the corresponding 1D cases: in Fig.4(b) a clear transition appears at $\epsilon = -98.5meV$ while the peak is located at $\epsilon = -89meV$ in the moderately weak coupling case of Fig. 4(d). In the antiadiabatic regime the main transitions are always due to the first addendum on the r.h.s. of eq.(7). We point out that also in the different context of the excitonic spectral function [45] the disappearance of side peaks in the absorption probability had been predicted in the antiadiabatic regime due to the fast phonon fluctuations which destroy the high-lying excited states in the potential well.

3. FINAL REMARKS

The Su-Schrieffer-Heeger tight binding model Hamiltonian has been extended to the study of a *two* dimensional electron-lattice structure. Through a perturbative approach and an exact computation of low order diagrams, we study the renormalization of the charge carrier effective mass versus the adiabaticity parameter both for a linear chain and for a square lattice. In the intermediate regime, where the phonons compete with the electrons on the energy scale, we find a sizeable mass enhancement which may be understood as a signature of polaron formation. This enhancement is more pronounced in the square lattice

mostly at $\omega_\pi \sim \sqrt{2}J$. The analysis of the electron spectral function shows that the model Hamiltonian hosts quite different behaviors according to the regime set by the adiabatic parameter. We have computed the spectral function at the bottom of the band in a number of representative cases by varying the strength of the effective coupling and using the spectral function sum rule as a testing bench for the reliability of our one phonon approximation. While in antiadiabatic conditions the electrons behave as good quasiparticles both in one and two dimensions, novel features emerge in the moderately adiabatic and intermediate regime where multiphononic terms become appreciable by increasing the strength of the *e-ph* coupling, the spectral weight is progressively spread among several transition peaks and the electronic quasiparticle picture is lost. Unlike the Holstein model whose ground state polaronic properties are essentially dimension independent, we find that the onset of a polaronic state is more likely to occur in 2D than in 1D thus confirming the trend of the effective mass computation and suggesting that the Su-Schrieffer-Heeger Hamiltonian is rather sensitive to dimensionality effects.

FIGURES

FIG. 1. Renormalized masses (in units of bare band electron mass) versus the adiabaticity parameter in one and two dimensions. $m_{eff}^{(1)}$ is due to the one phonon self-energy correction. The coupling constants are in meV.

FIG. 2. 1D and 2D Electron spectral functions in the adiabatic regime and (a,b) extremely weak *e-ph* coupling; (c,d) moderately weak *e-ph* coupling. $J = 0.1eV$.

FIG. 3. 1D and 2D Electron spectral functions in the intermediate regime and (a,b) extremely weak *e-ph* coupling; (c,d) moderately weak *e-ph* coupling. $J = 0.1eV$.

FIG. 4. 1D and 2D Electron spectral functions in antiadiabatic regime and (a,b) extremely weak *e-ph* coupling; (c,d) moderately weak *e-ph* coupling. $J = 0.1eV$.

ACKNOWLEDGEMENTS

This work has been done at the Coop "Il Rafano" in Trequanda.

REFERENCES

[1] L.D Landau, Z.Phys. **3** (1933) 664; L.D.Landau, S.I.Pekar, Zh.Eksp.Teor.Fiz. **16** (1946) 341.

[2] Y.Toyozawa, Prog. Theor. Phys. **26** (1961) 29.

[3] D.M.Eagles, Phys. Rev. **145** (1966) 645.

[4] D.Emin, T.Holstein, Phys. Rev. Lett. **36** (1976) 323.

[5] J.T.Devreese, *Polarons* in Encyclopedia of Applied Physics (VCH Publishers, NY) **14** (1996) 383.

[6] A.H.Romero, D.W.Brown, K.Lindenberg, Phys. Rev. B **59** (1999) 13728.

[7] E.V.L.de Mello, J.Ranninger, Phys. Rev. B **58** (1998) 9098.

[8] H.Fehske, H.Röder, G.Wellein, A.Mistriotis, Phys. Rev. B **51** (1995) 16582.

[9] A.S.Alexandrov, N.F.Mott, Rep. Prog. Phys. **57** (1994) 1197; A.S.Alexandrov, A.B.Krebs, Sov. Phys. Usp. **35** (1992) 345.

[10] E.I.Rashba, in *Excitons*, Rashba and Sturge eds., North-Holland, Amsterdam 1982.

[11] H.De Raedt, A.Lagendijk, Phys. Rev. B **27** (1983) 6097.

[12] G.Kopidakis, C.M.Soukoulis, E.N.Economou, Phys. Rev. B **51** (1995) 15038.

[13] G.Kalosakas, S.Aubry, G.P.Tsironis, Phys. Rev. B **58** (1998) 3094.

[14] A.H.Romero, D.W.Brown, K.Lindenberg, Phys. Rev. B **60** (1999) 14080.

[15] P.E.Kornilovitch, E.R.Pike, Phys. Rev. B **55** (1997) R8634.

[16] E.Jeckelmann, S.R.White, Phys. Rev. B **57** (1998) 6376.

[17] B.Gerlach, H.Löwen, Rev. Mod. Phys. **63** (1991) 63.

[18] K.Yonemitsu, Phys. Rev. B **50** (1994) 2899.

[19] A.S.Alexandrov, V.V.Kabanov, D.K.Ray, Phys. Rev. B **49** (1994) 9915.

[20] M.Zoli, J.Phys.:Condens.Matter **13** (2001) 10845.

[21] T.Holstein, Ann. Phys. (N.Y.) **8** (1959) 325.

[22] Acoustical polarons have been studied also in the framework of the Fröhlich Hamiltonian. See, G.A.Farias, W.B.da Costa, F.M.Peeters, Phys. Rev. B **54** (1996) 12835.

[23] M.Zoli, Phys. Rev. B **61** (2000) 14523.

[24] M.Zoli, Physica C **324** (1999) 71.

[25] S.Barisic, Phys. Rev. B **5** (1972) 932.

[26] H.J.Schulz, Phys. Rev. B **18** (1978) 5756.

[27] Y.Lu, *Solitons and Polarons in Conducting Polymers* World Scientific, Singapore 1988.

[28] A.J.Heeger, S.Kivelson, J.R.Schrieffer, W.P.Su, Rev. Mod. Phys. **60** (1988) 781.

[29] W.P.Su, J.R.Schrieffer, A.J.Heeger, Phys. Rev. Lett. **42** (1979) 1698.

[30] H.Takayama, Y.R.Lin-Liu, K.Maki, Phys. Rev. B **21** (1980) 2388.

[31] While quantum fluctuations destroy the dimerization order in the case of spinless electrons below a critical value of electron-phonon coupling, the dimerized ground state always survives for a spin- 1/2 electron system. See, J.E.Hirsch, E.Fradkin, Phys. Rev. Lett. **49** (1982) 402; Phys. Rev. B **27** (1983) 1680. In the presence of electron-electron interactions (SSH-Hubbard model) both the charge and spin gap opening have been studied by K.Yonemitsu, M.Imada, Phys. Rev. B **54** (1996) 2410.

[32] D.K.Campbell, A.R.Bishop, Phys. Rev. B **24** (1981) 4859.

[33] Y.Onodera, S.Okuno, J.Phys.Soc.Jpn. **52** (1983) 2478.

[34] Unlike solitons, polarons are not associated with the degenerate ground state. They can

provide the fundamental excitations in nondegenerate polymers: see, D.Boyanovsky, C.A.A. de Carvalho, E.S.Fraga, Phys. Rev. B **50** (1994) 2889.

[35] B.Horowitz, Phys. Rev. Lett. **46** (1981) 742.

[36] S.Kivelson, A.J.Heeger, Phys. Rev. Lett. **55** (1985) 308.

[37] S.Tang, J.E.Hirsch, Phys. Rev. B **37** (1988) 9546.

[38] Y.Ono, T.Hamano, J.Phys.Soc.Jpn. **69** (2000) 1769.

[39] N.Miyasaka, Y.Ono, J.Phys.Soc.Jpn. **70** (2001) 2968.

[40] P.A.Khomyakov, Phys. Rev. B **63** (2001) 153405.

[41] M.Nakahara, K.Maki, Phys. Rev. B **25** (1982) 7789.

[42] G.D.Mahan, *Many Particle Physics*, Plenum Press, N.Y. (1981) 107.

[43] J.M.Robin, Phys. Rev. B **56** (1997) 13634.

[44] A broad absorption background may be partly due to electron-electron interactions in strongly correlated systems. See, e.g., T.Timusk, B.Statt, Rep. Prog. Phys. **62** (1999) 61.

[45] A.Kongeter, M.Wagner, J.Chem.Phys. **92** (1990) 4003.

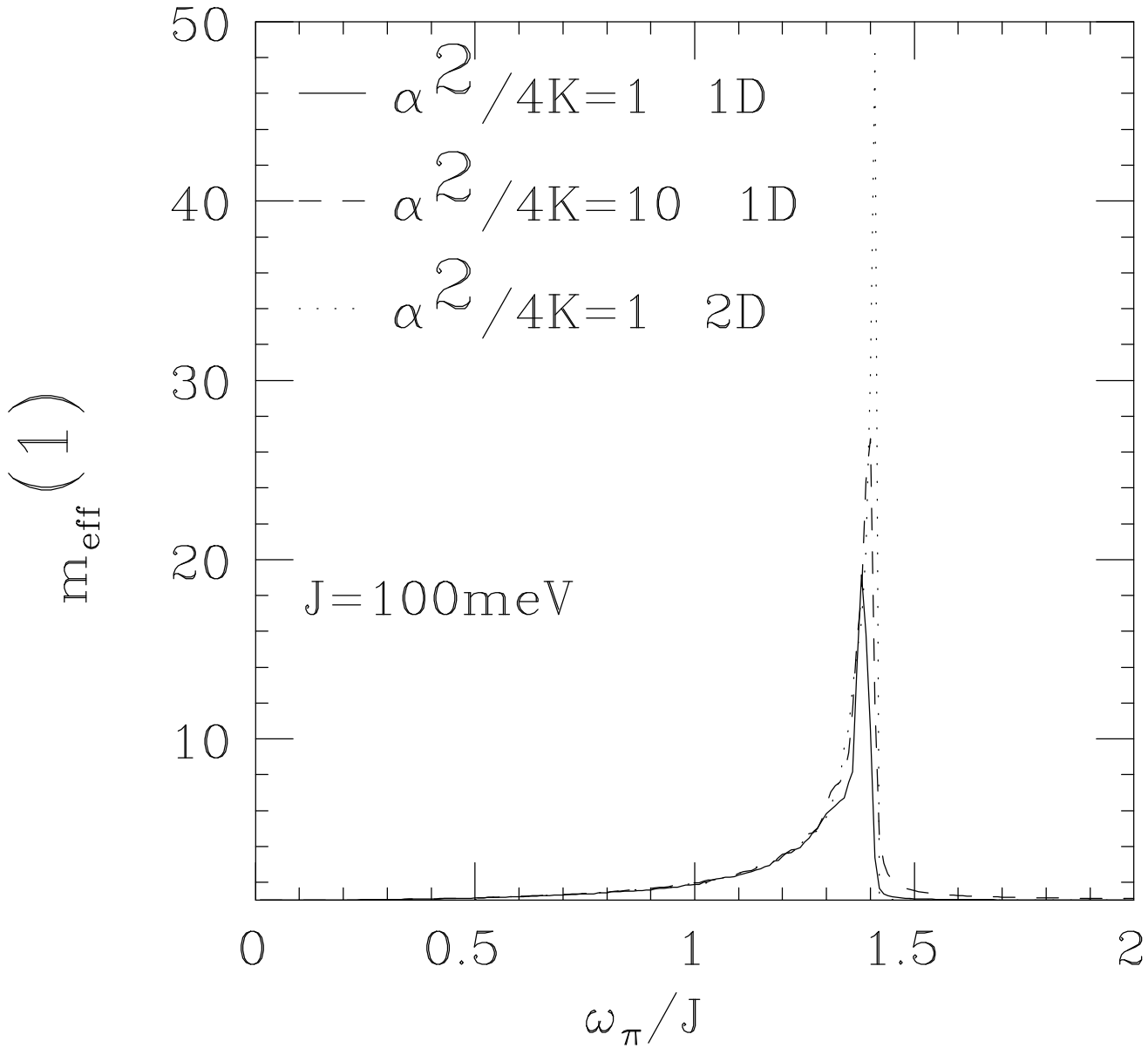
50
40
30
20
10
0
0.5
1
1.5
2
$m_{eff}(1)$
ω_π/J
$\alpha^2/4K=1$ 1D
$\alpha^2/4K=10$ 1D
$\alpha^2/4K=1$ 2D
J=100meV

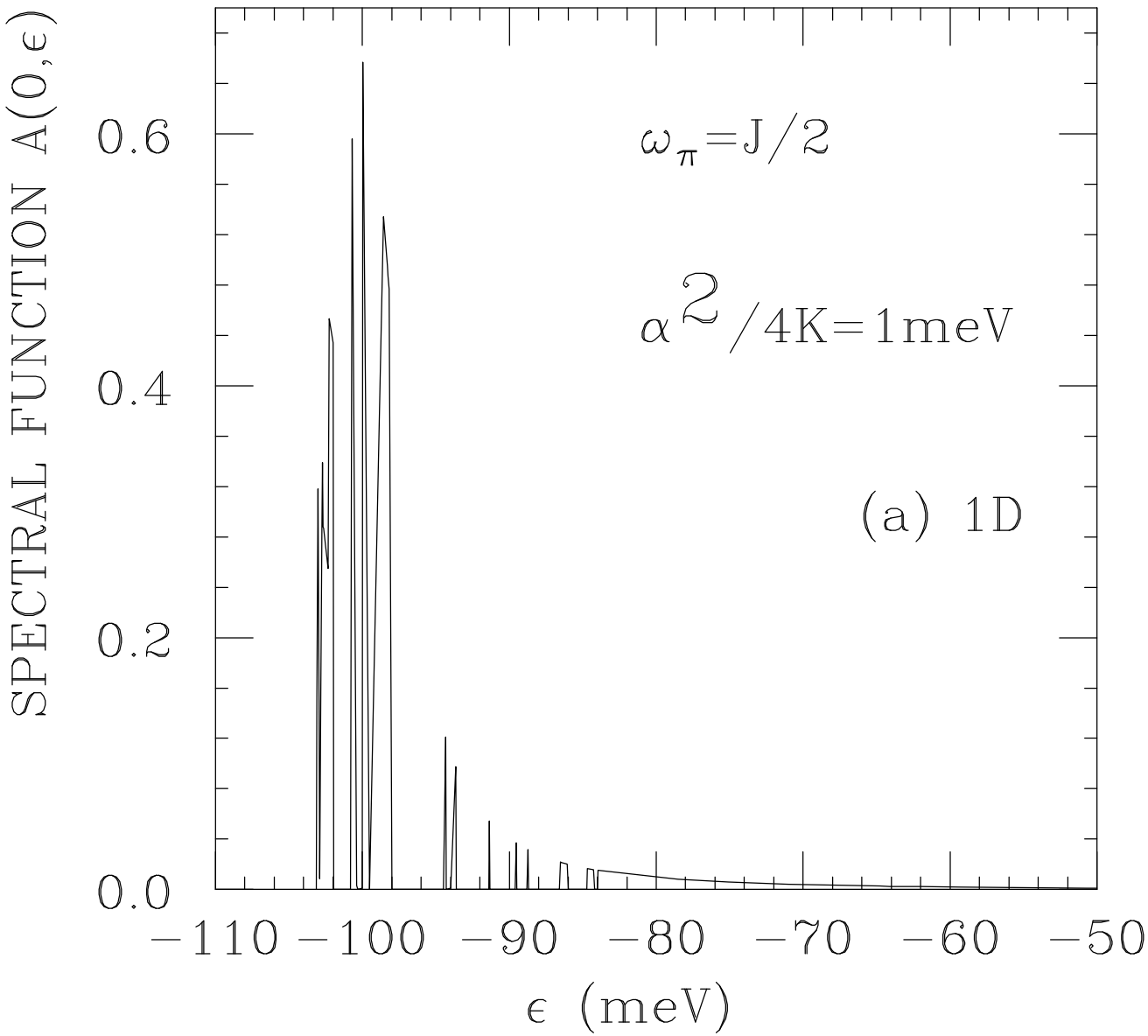
SPECTRAL FUNCTION A(0,ϵ)
0.0
0.2
0.4
0.6
−110
−100
−90
−80
−70
−60
−50
ϵ (meV)
ω_π=J/2
α^2/4K=1meV
(a) 1D

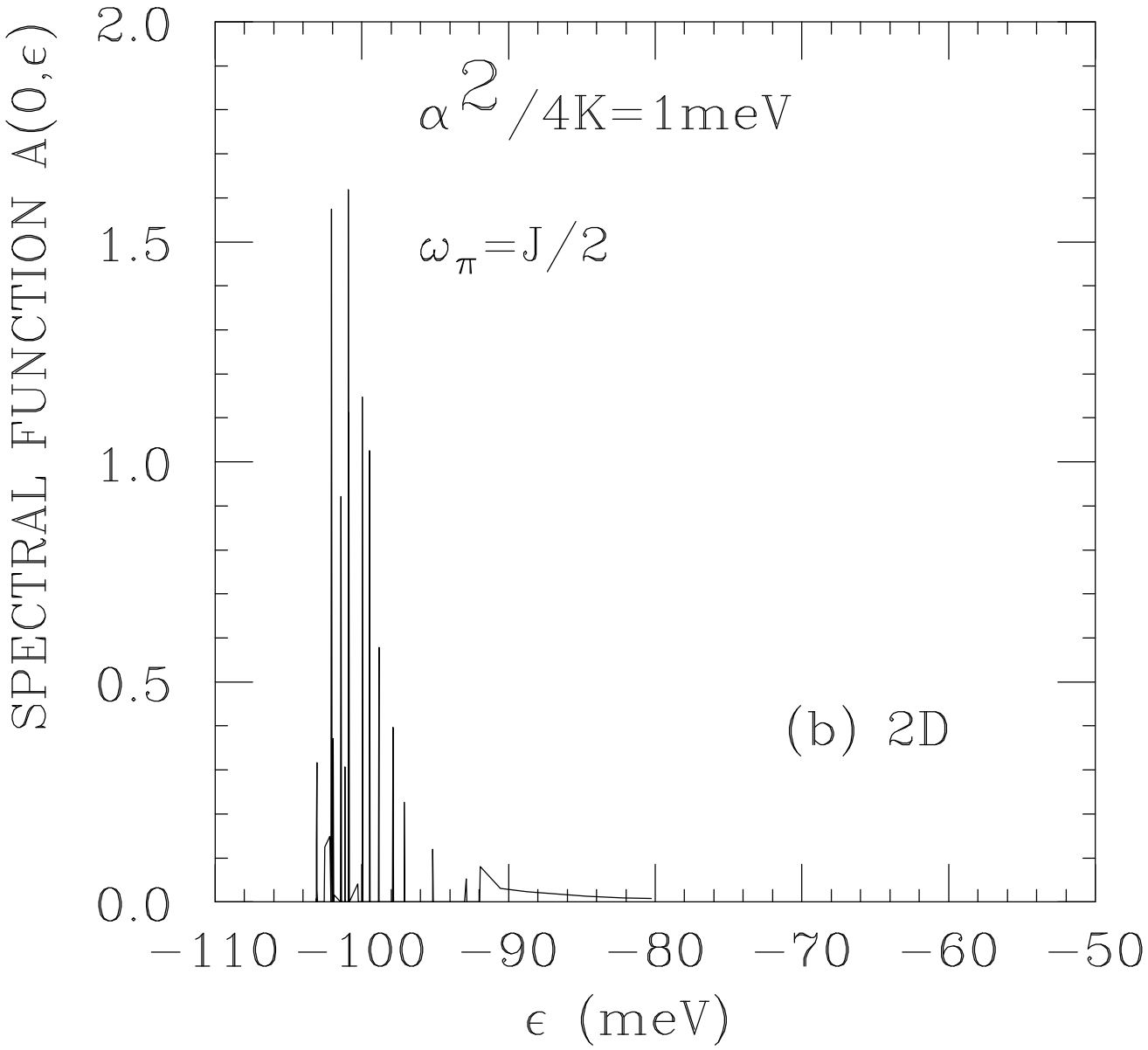
SPECTRAL FUNCTION A(0,ϵ)
2.0
1.5
1.0
0.5
0.0
α²/4K=1meV
ω_π=J/2
(b) 2D
−110
−100
−90
−80
−70
−60
−50
ϵ (meV)

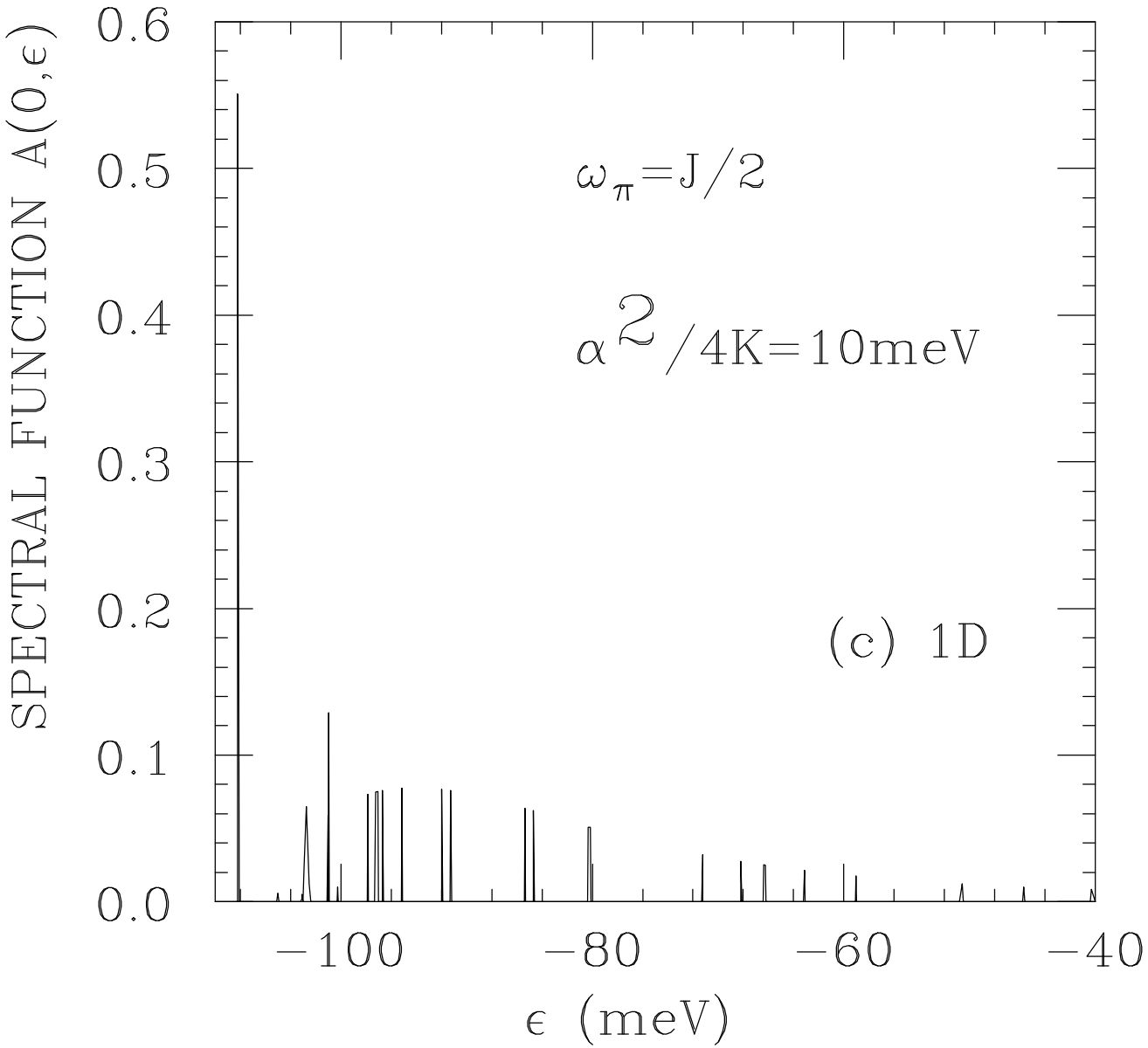
SPECTRAL FUNCTION A(0,ϵ)
0.6
0.5
0.4
0.3
0.2
0.1
0.0
ω_π=J/2
α^2/4K=10meV
(c) 1D
−100
−80
−60
−40
ϵ (meV)

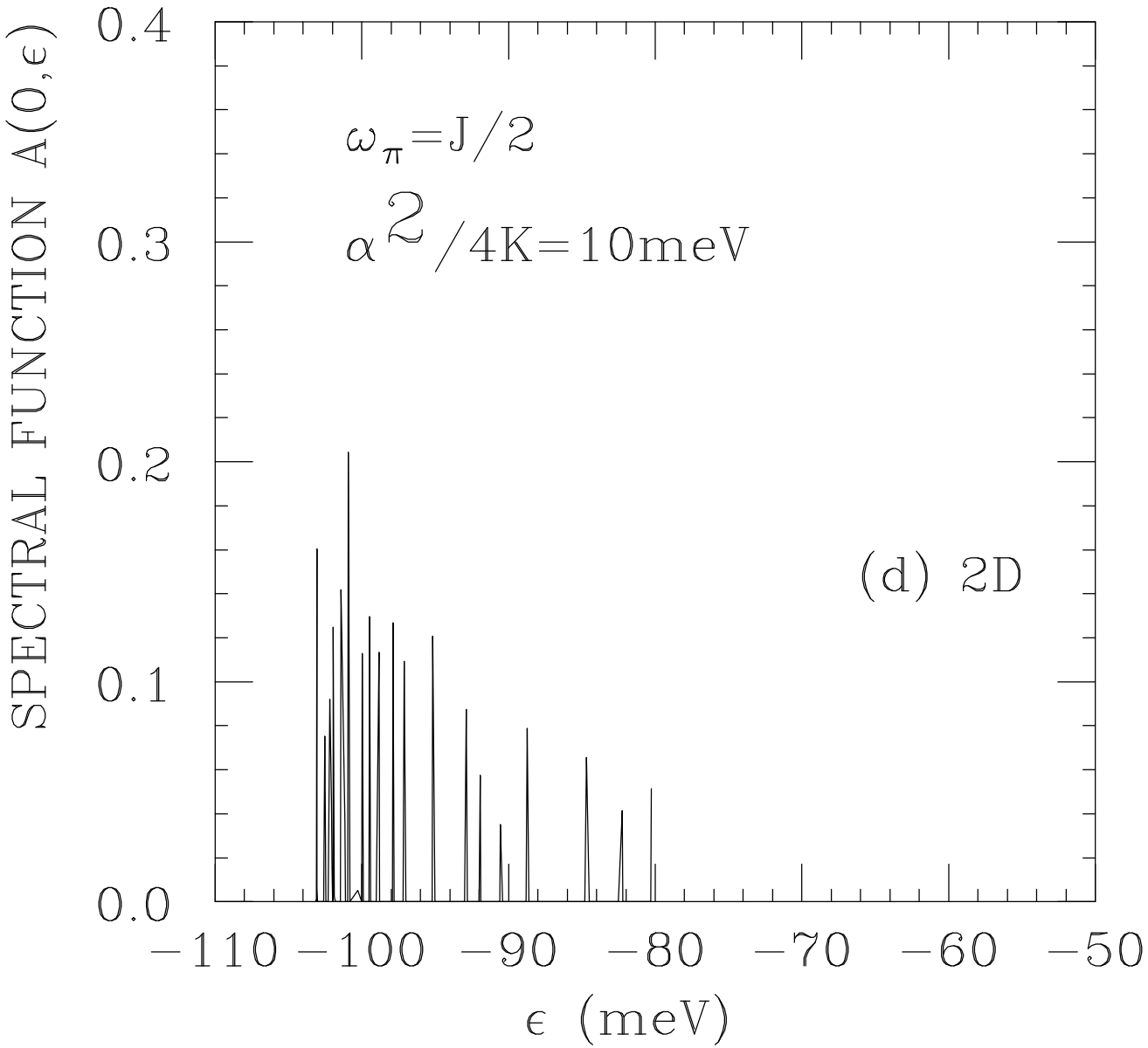
SPECTRAL FUNCTION A(0,ϵ)
0.4
0.3
0.2
0.1
0.0
ω_π=J/2
α^2/4K=10meV
(d) 2D
−110
−100
−90
−80
−70
−60
−50
ϵ (meV)

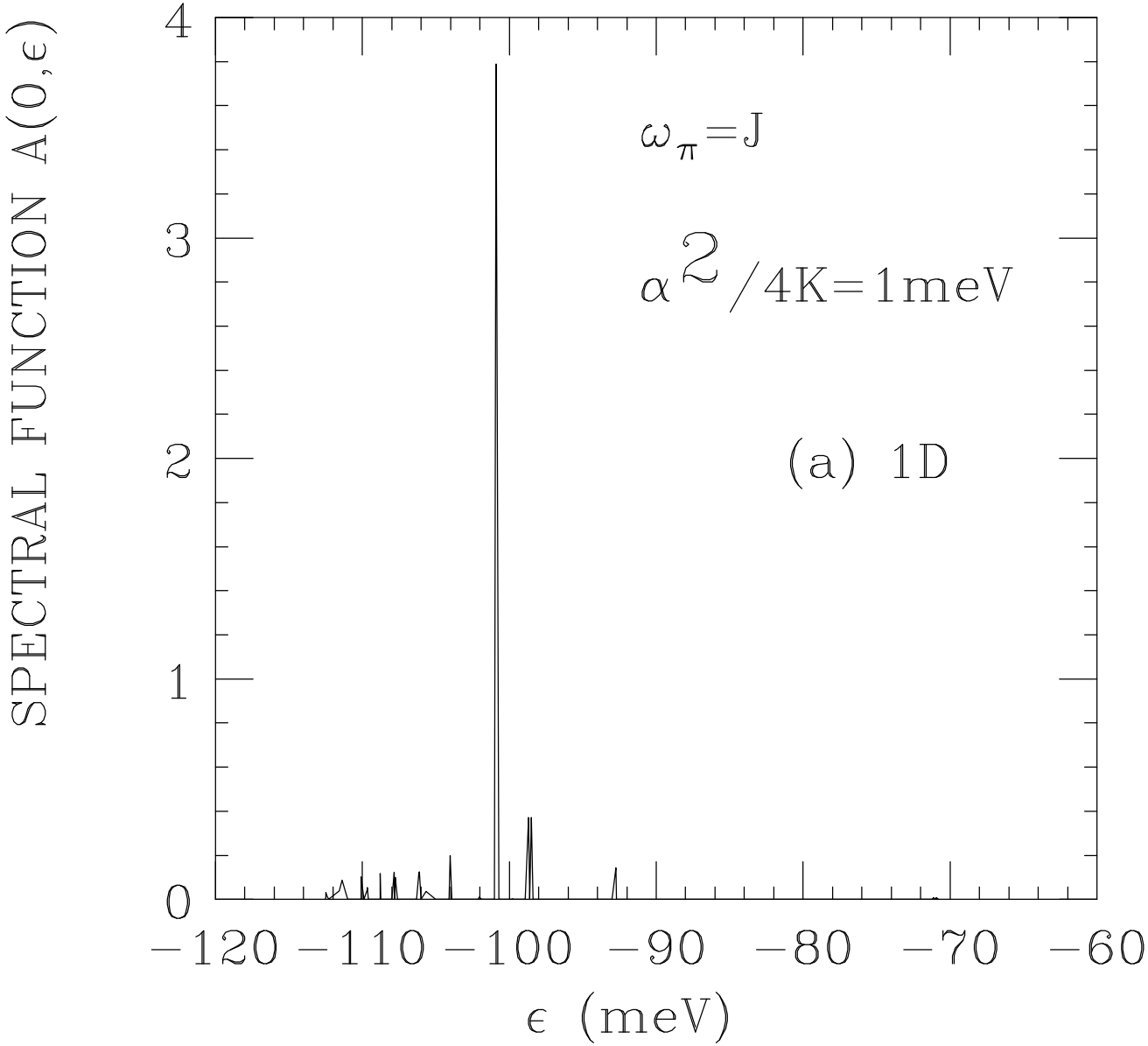
SPECTRAL FUNCTION A(0,ϵ)
4
3
2
1
0
ω_π=J
α^2/4K=1meV
(a) 1D
−120
−110
−100
−90
−80
−70
−60
ϵ (meV)

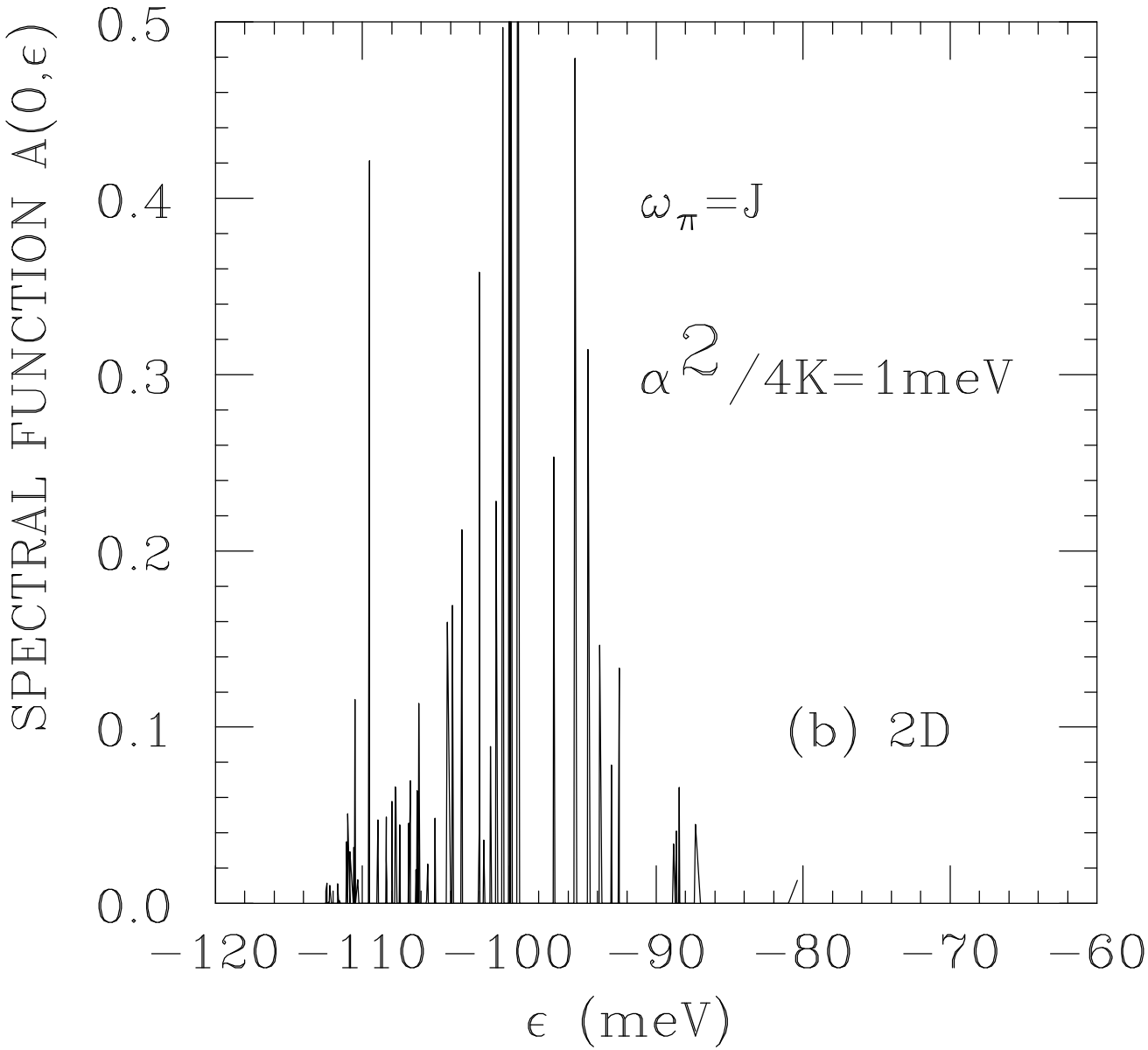
SPECTRAL FUNCTION A(0,ϵ)
0.5
0.4
0.3
0.2
0.1
0.0
−120 −110 −100 −90 −80 −70 −60
ϵ (meV)
ω_π=J
α^2/4K=1meV
(b) 2D

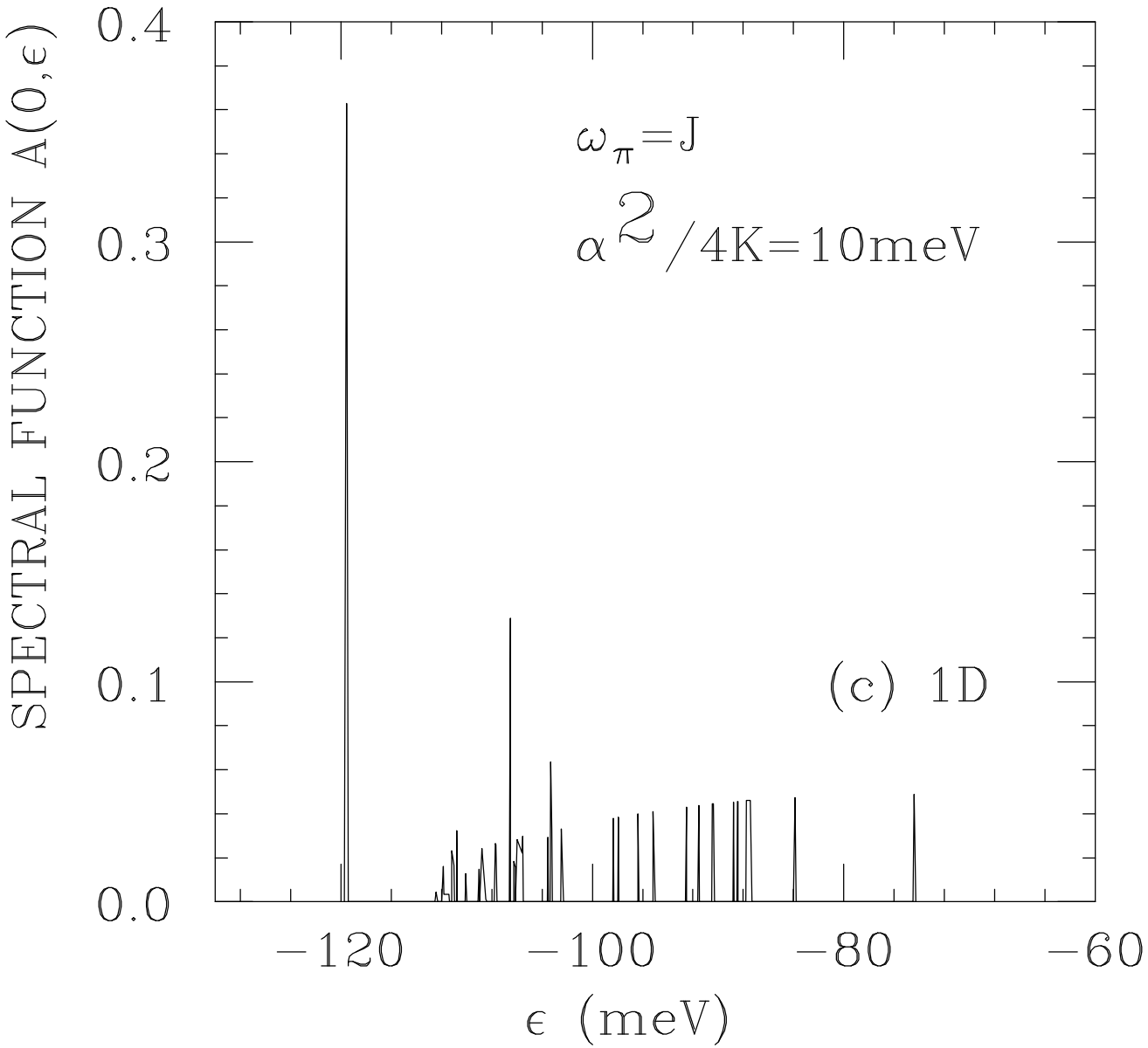
SPECTRAL FUNCTION A(0,ϵ)
0.4
0.3
0.2
0.1
0.0
−120
−100
−80
−60
ϵ (meV)
ω_π=J
α^2/4K=10meV
(c) 1D

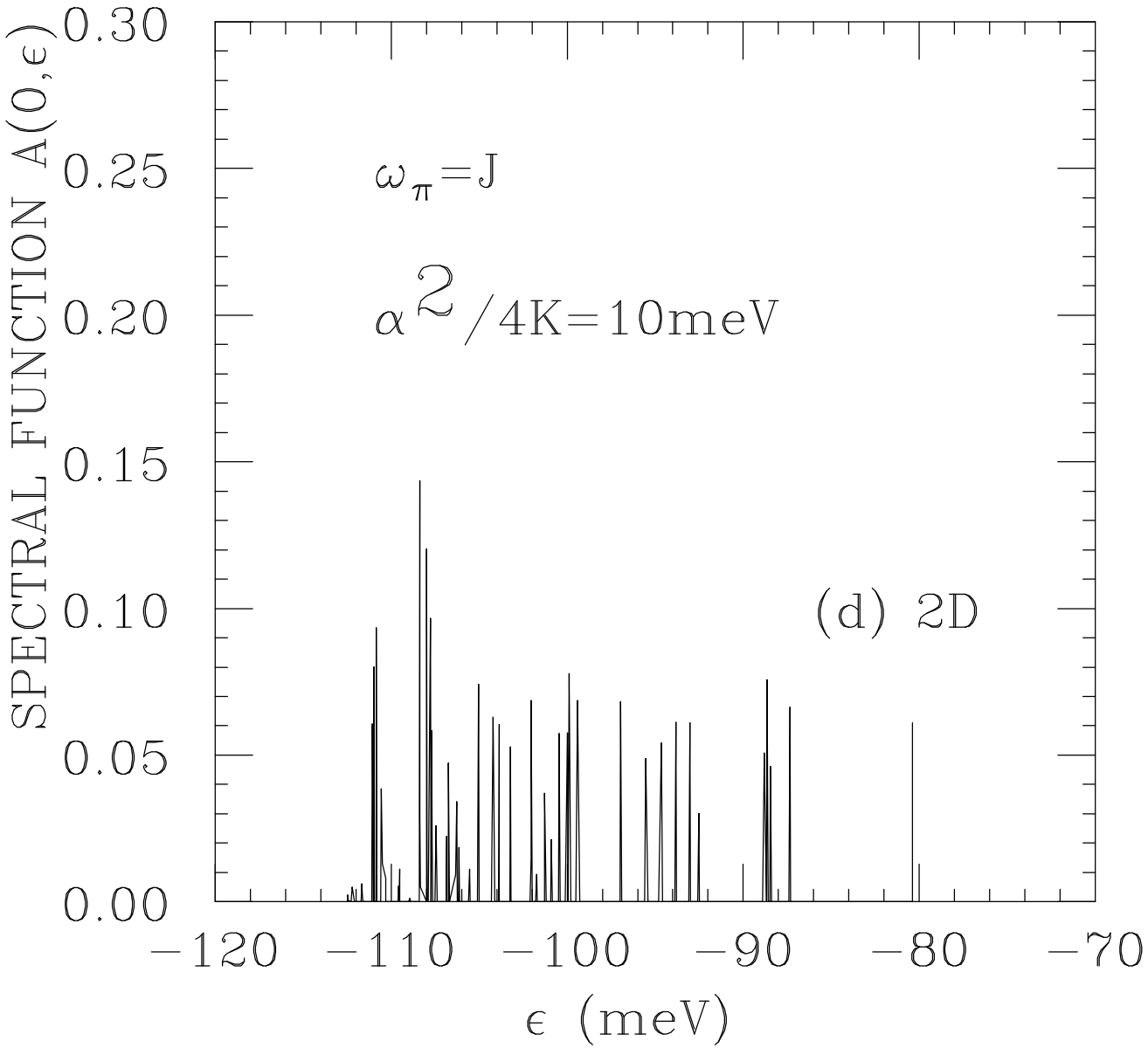
SPECTRAL FUNCTION A(0,ϵ)
0.30
0.25
0.20
0.15
0.10
0.05
0.00
ω_π=J
α^2/4K=10meV
(d) 2D
−120
−110
−100
−90
−80
−70
ϵ (meV)

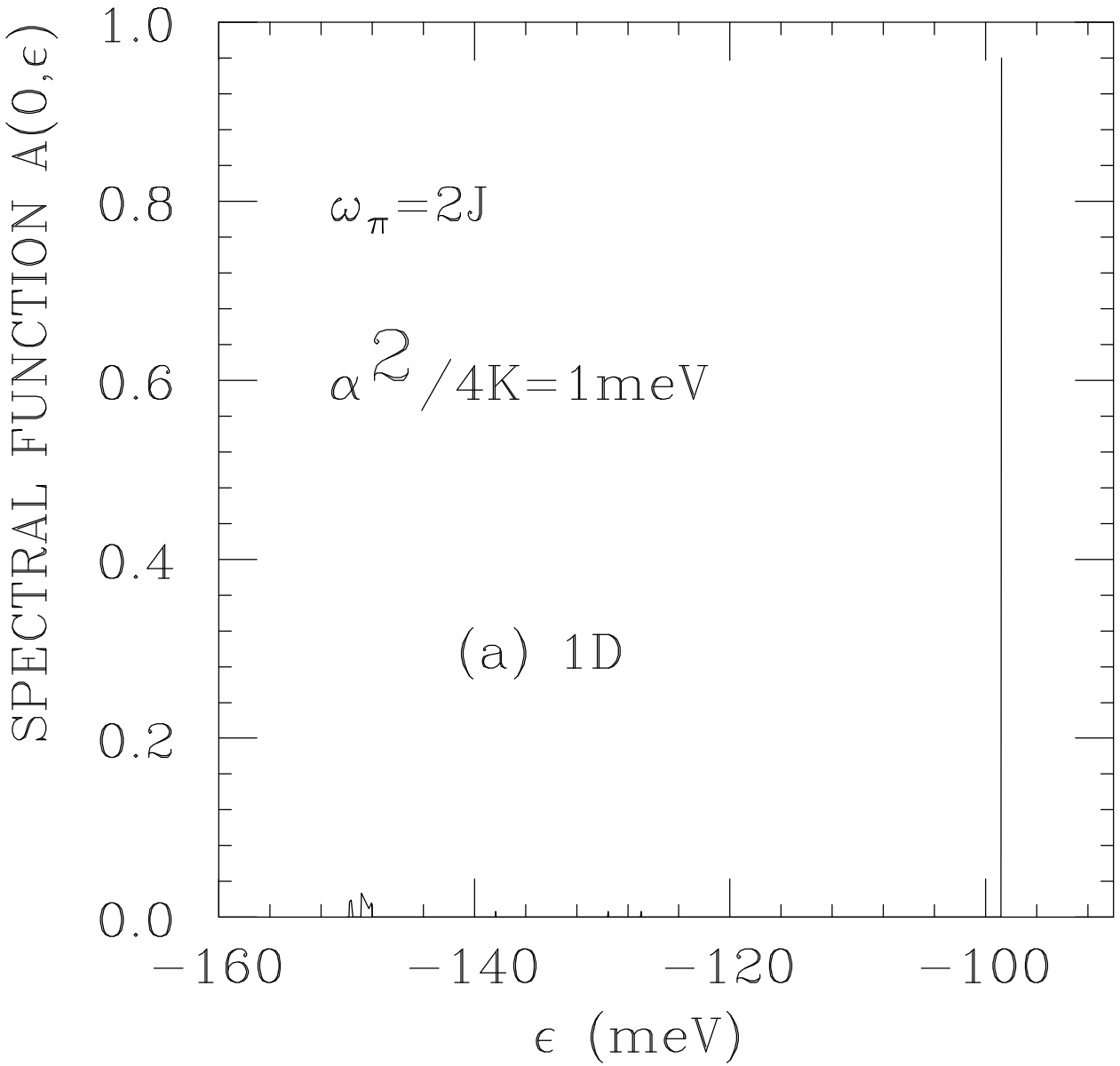
SPECTRAL FUNCTION A(0,ϵ)
1.0
0.8
0.6
0.4
0.2
0.0
−160
−140
−120
−100
ϵ (meV)
ω_π=2J
α^2/4K=1meV
(a) 1D

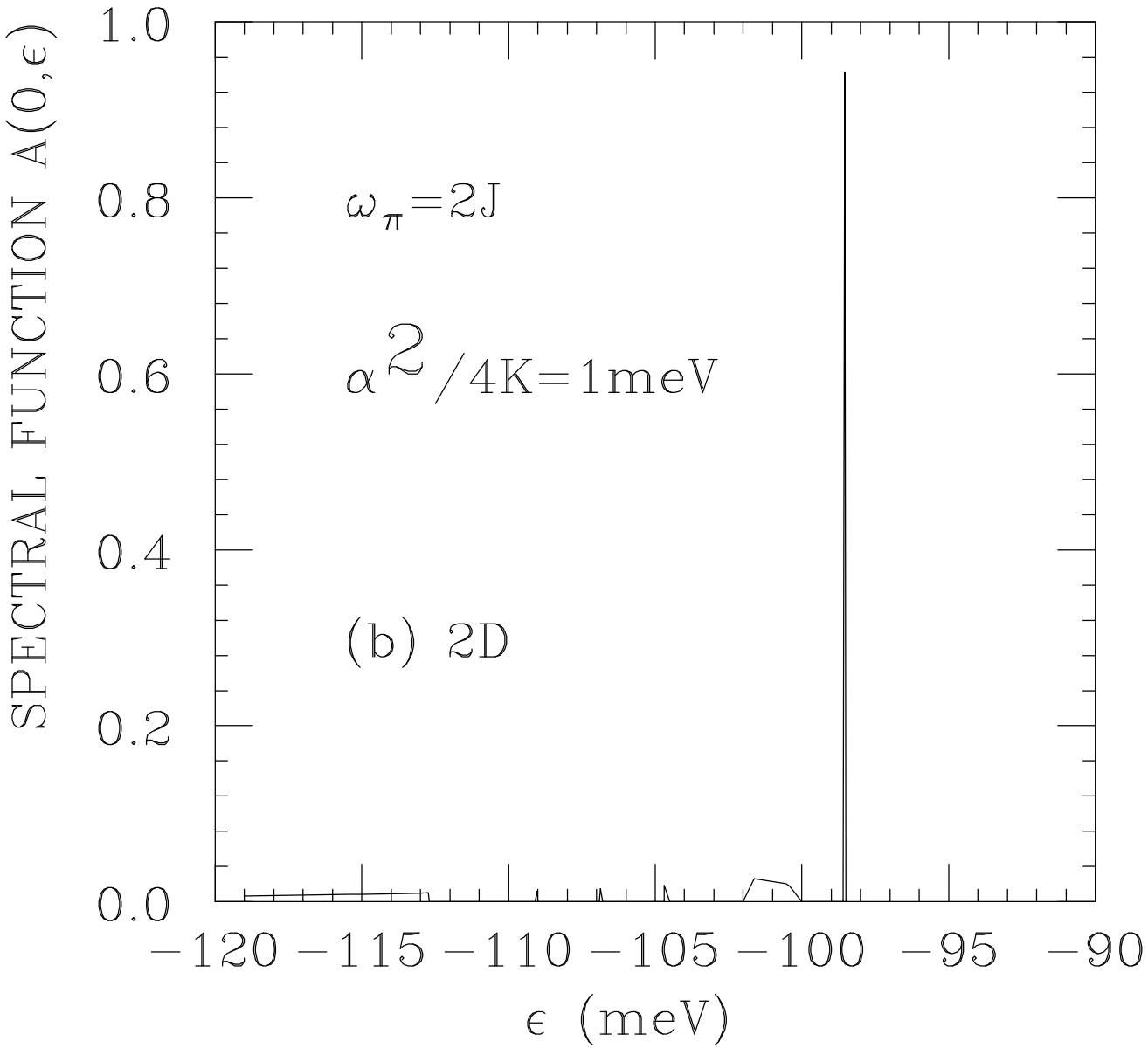
SPECTRAL FUNCTION A(0,ϵ)
1.0
0.8
0.6
0.4
0.2
0.0
ω_π=2J
α^2/4K=1meV
(b) 2D
−120 −115 −110 −105 −100 −95 −90
ϵ (meV)

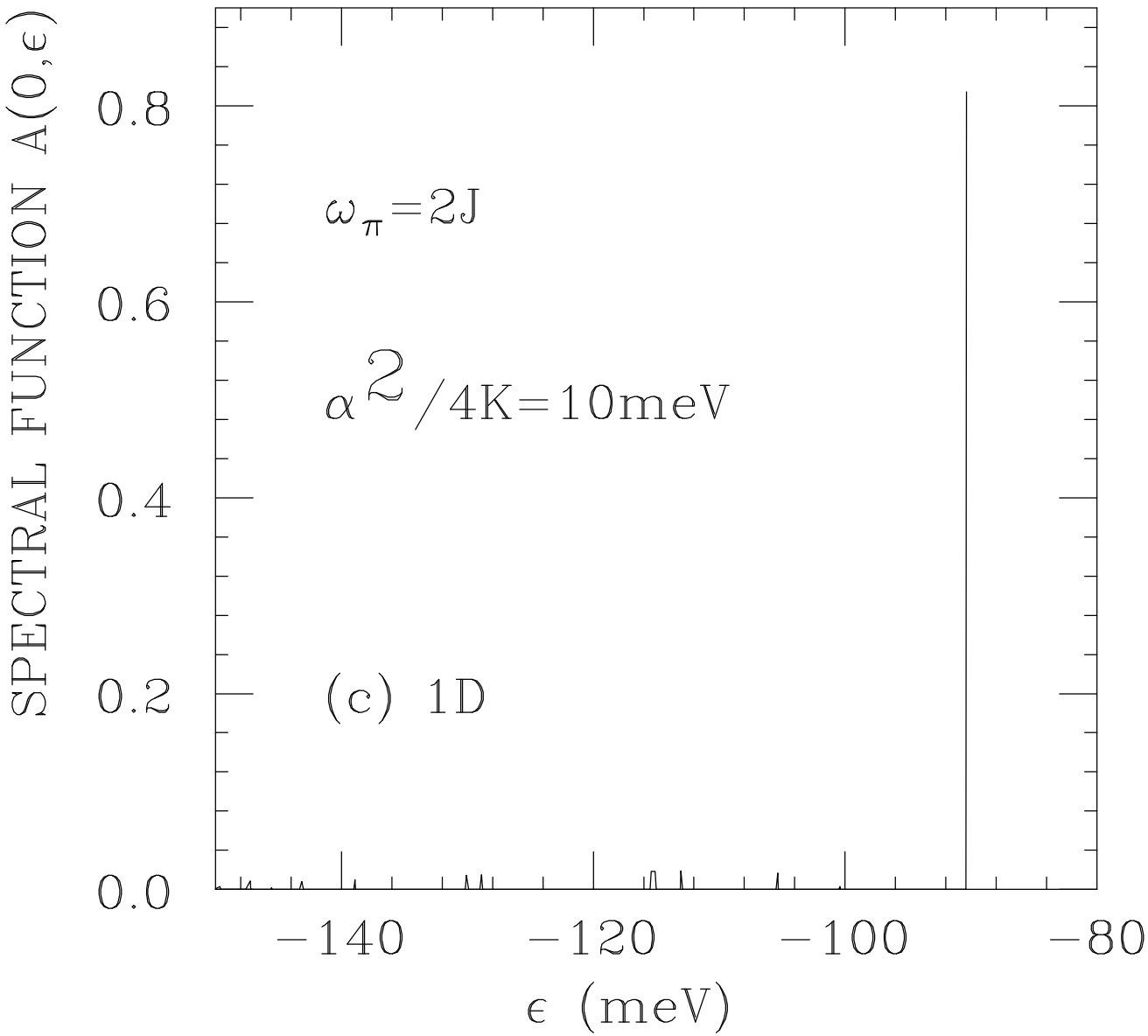
SPECTRAL FUNCTION A(0,ϵ)
0.0
0.2
0.4
0.6
0.8
ω_π=2J
α^2/4K=10meV
(c) 1D
−140
−120
−100
−80
ϵ (meV)

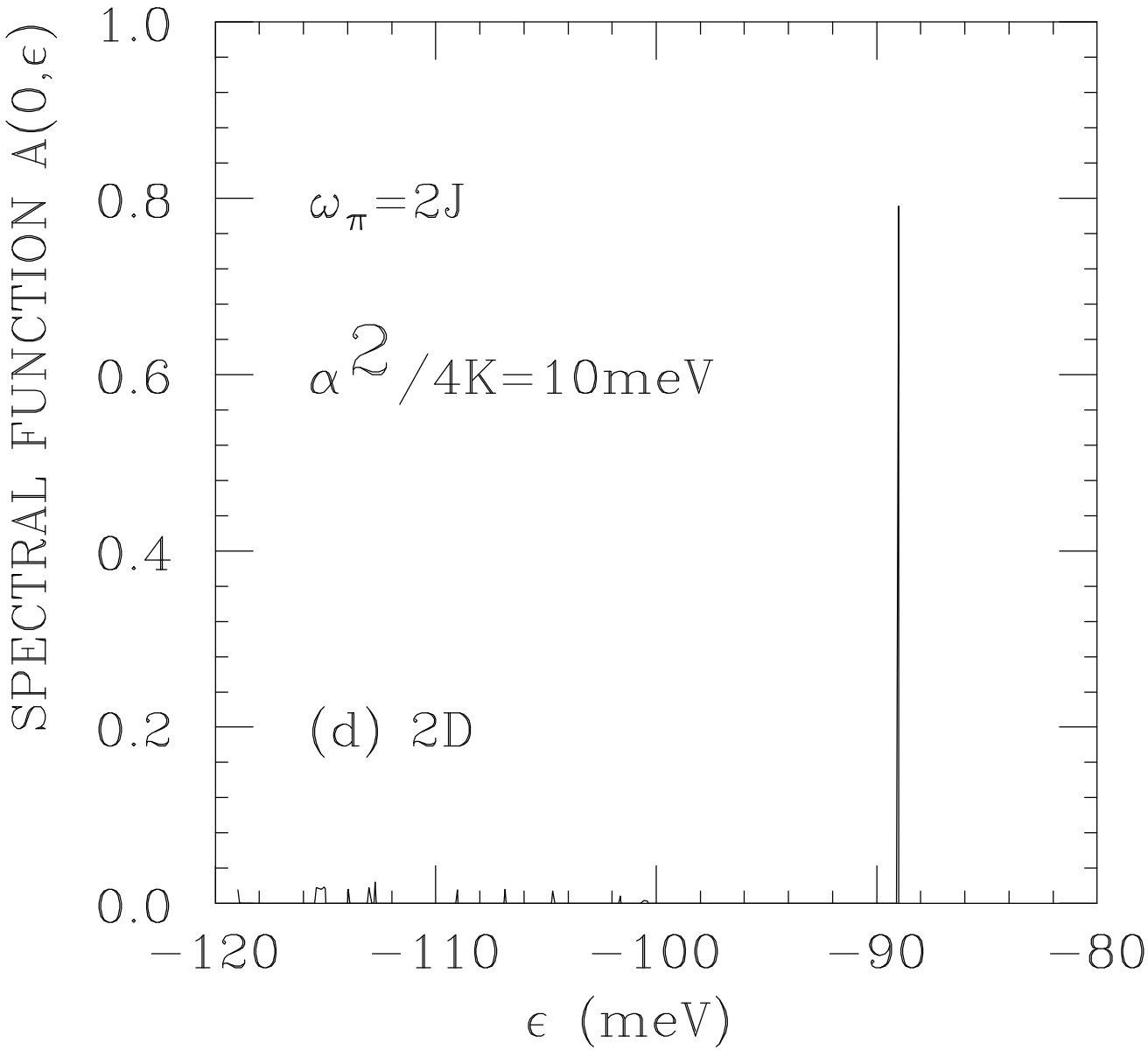
SPECTRAL FUNCTION A(0,ϵ)
1.0
0.8
0.6
0.4
0.2
0.0
ω_π=2J
α²/4K=10meV
(d) 2D
−120
−110
−100
−90
−80
ϵ (meV)